International Journal of Engineering and Advanced Technology (IJEAT)
ISSN: 2249-8958 (Online), Volume-9 Issue-1, October, 2019

A Mathematical Framework for Modelling of Current Source Converter Based High Voltage DC Transmission Systems

S.Seenivasan, S.Vadivel

Abstract*: Transmission of electrical power through High Voltage Direct Current (HVDC) has attracted the attention of several researchers in the recent years. To investigate the performance of HVDC transmission systems, a complete linear mathematical model is required. In this paper, a well-developed linear continuous model of current source converter based twelve pulse HVDC transmission systems is presented. In which, the converter AC system is represented by damped LLR equivalents at fundamental frequency and at the third harmonic. Also, they are equipped with double tuned harmonic filter and second order high pass filter to suppress the AC harmonics and a capacitor for reactive power compensation. The DC system is secured with rectifier current control, inverter current control, inverter voltage control and inverter extinction angle control. The HVDC transmission system model is implemented in the MATLAB/Simulink environment and the performance of the system has been investigated by observing the rectifier side AC quantities, rectifier DC quantities, inverter side AC quantities and inverter DC quantities.

Keywords*: DC control, Double tuned filter, HVDC transmission systems, Linear state space model, Steady state operation.

I. INTRODUCTION

The power transmission through HVDC technology is now mature and experiencing rapid increases in the voltage, power carrying capacity and length of transmission lines [1]. While comparing with three phase HVAC transmission systems, HVDC transmission system is commendable in the following portions: (i) HVDC transmission line cost and operating cost are less (ii) it need not operate synchronously between two AC systems linked by HVDC and (iii) it is simple to control and adjust the power flow [2]. HVDC technology finds application in the transmission of power over long unbroken overland distances, significant underwater distances, and in the interconnection of separate, or partitioned, AC systems [3]. HVDC transmission system is composed of three major parts: a) rectifier station to convert AC to DC, b) transmission link and c) inverter station to convert back to AC [4]. Most of the HVDC systems have current source converters.

Revised Manuscript Received on October 30, 2019.
* Correspondence Author
Dr.S.Seenivasan, Dept of EEE, Government College of Engineering, Dharmapuri-636 704, Tamilnadu, India.. Email: svan4284@gmail.com
Dr.S.Vadivel, Dept of EEE, Government Polytechnic College, Ariyalur-621 707, Tamilnadu, India. Email: vadivels85@gmail.com

By means of filter and/or capacitor banks connected on the primary side of the converter transformer, the reactive power is supplied. Various control techniques are employed for the control and protection of the line and converter against faults [5] [6] [7].

The CIGRE benchmark HVDC transmission system model [8] is projected for comparison of different simulation methods and results, which are also especially related to control strategies and recovery routine studies. A linear continuous analytical model based on the CIGRE benchmark system is derived in [9] for the investigation of most of the practically observed issues related with the operation of HVDC systems. The importance of that model are the second harmonic instability and the problems related to the low SCR AC systems connected to a DC system. In that model rectifier side is equipped with current control and the actual controller for inverter are not taken in to account instead of that constant beta control is considered. In actual practice the appropriate firing angle is determined by considering the involvement of various inverter controls. So, following the similar modelling procedure a linear continuous mathematical model of current source converter based twelve pulse HVDC transmission system is presented in this paper. In which the AC system is represented as damped LLR equivalent and the AC filter consists of capacitor banks to supply the reactive power compensation required, double tuned harmonic filter and damped high pass filter to mitigate the AC harmonics. The DC system is defended with rectifier current control, inverter current control, inverter voltage control and inverter extinction angle control. The HVDC transmission system model is developed in the MATLAB/Simulink environment. The operation of the system has been validated by observing the rectifier side AC quantities, rectifier DC quantities, inverter side AC quantities and inverter DC quantities.

The rest of the paper is organized as follows: section 2 addresses the modelling of current source converter based HVDC transmission system with enough mathematical illustrations. Section 3 details our simulation results and discussion. Finally, conclusions are given in section 4.

II. MODELLING OF HVDC TRANSMISSION SYSTEM

The 12-pulse current source converter based monopolar HVDC transmission system shown in the Fig. 1. is used for the model advancement.

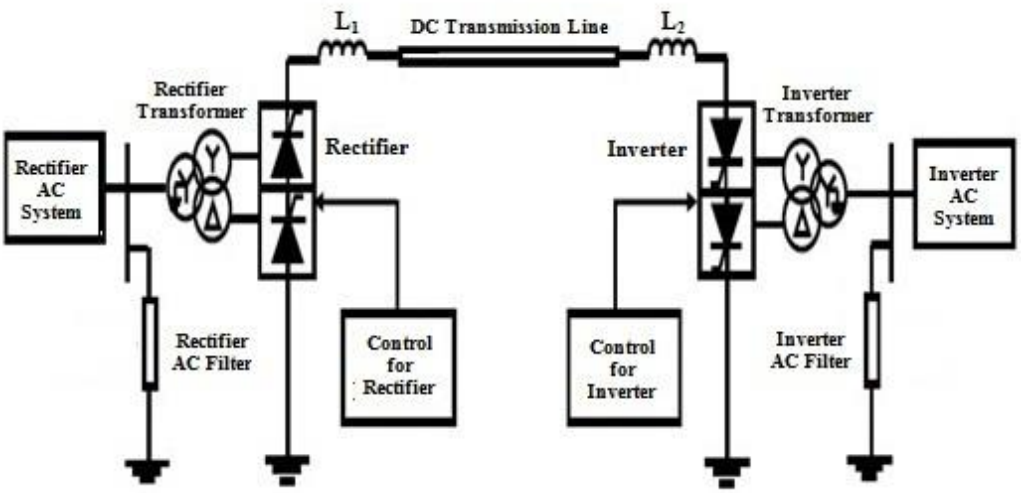

Fig. 1. The HVDC transmission system model

A. Modelling of DC network

In general, the DC network consists of smoothing reactor, DC filters and the transmission line. Neglecting DC filters, the DC line is modelled as a T equivalent. A monopolar line with ground return which is terminated by converters stations with two six pulse bridge in each station. The rectifier is protected by means of current controller alone, but the inverter is safeguarded with current control, voltage control and extinction angle control. The s-domain equivalent of state equations representing the complete DC network considering the linearized direct voltages, rectifier current control, inverter current control, inverter voltage control, inverter extinction angle control [10] is given by,

$$sX_1L_{DCLR} = -X_1R_{DCLR} + K_{ACR}X_{16} - K_{EACR}E_{ACR} + K_{EACR}E_{ACRD} - X_7 \quad (2.1)$$

Where, the state X_1 in the above equation represents the current flowing in the rectifier side DC link(I_{DCLR}).

The total inductance at the rectifier terminals is given by $L_{DCLR} = L_{AVTR} + L_1 + 0.5L_{DCL}$, which includes the averaged rectifier transformer reactance, the smoothing reactor and the DC line inductance,

The total resistance at the rectifier terminal is given by $R_{DCLR} = R_{CRR} + R_1 + 0.5R_{DCL}$, which includes the commutating overlap equivalent resistance at rectifier side, the internal resistance of the smoothing reactor and the DC line resistance,

The linearized coefficients K_{ACR}, K_{EACR} and R_{CRR} are obtained from the non-linear rectifier direct voltage equation given by, $V_{DCLR} = 6E_{ACR}\sqrt{2}\varphi_{DCR}/\pi + (3/\pi)X_{CRR}I_{DCLR}$

X_{CRR} is equivalent rectifier transformer reactance at fundamental frequency,

E_{ACR} is rectifier AC commutating voltages ($E_{ACR} = K_{TR}V_{ACR}$ where $K_{TR}$is for transformer ratio),

φ_{DCR} is the appropriate firing angle of rectifier,

E_{ACRD} is rectifier AC voltage disturbance.

$$sX_2 = K_{IIR}X_{12} - K_{IIR}I_{REF} \quad (2.2)$$

Where, the state X_2 in the above equation represents the output from the integral part of the rectifier PI current controller,

K_{IIR} is the rectifier current controller integral gain,

I_{IRF} is the rectifier direct current feedback signal,

I_{REF} is the current reference as an external input.

$$sX_4L_{DCLI} = -X_1R_{DCLI} + X_7 - K_{SI}X_{19} - K_{ESI}E_{SI} + K_{ESI}E_{SID} \quad (2.3)$$

Where, the state X_4 in the above equation represents the current flowing in the inverter side DC link(I_{DCLI}).

The total inductance at the inverter terminals is given by $L_{DCLI} = L_{AVTI} + L_2 + 0.5L_{DCL}$, which includes the averaged inverter transformer reactance, the smoothing reactor and the DC line inductance,

The total resistance at the inverter terminal is given by $R_{DCLI} = R_{CRI} + R_2 + 0.5R_{DCL}$, which includes the commutating overlap equivalent resistance at inverter side, the internal resistance of the smoothing reactor and the DC line resistance,

The linearized coefficients K_{ACI}, K_{EACI} and R_{CRI} are obtained from the non-linear inverter direct voltage equation given by $V_{DCLI} = 6E_{ACI}\sqrt{2}\varphi_{DCI}/\pi + (3/\pi)X_{CRI}I_{DCLI}$

X_{CRI} is equivalent inverter transformer reactance at fundamental frequency.

E_{ACI} is inverter AC commutating voltages ($E_{ACI} = K_{TI}V_{ACI}$ where $K_{TI}$is for transformer ratio),

φ_{DCI} is the appropriate firing angle of inverter,

E_{ACID} is inverter AC voltage disturbance.

$$sX_4 = K_{III}X_{13} - K_{III}I_{REF} + K_{III}I_{MAR} \quad (2.4)$$

Where,

the state X_4 in the above equation represents the output from the integral part of the inverter PI current controller,

K_{III} is the inverter current controller integral gain,

I_{IRF} is the inverter direct current feedback signal,

I_{MAR} is the current margin as an external input.

$$sX_5 = -K_{VII}X_{14} + K_{VII}V_{REF} - K_{VII}V_{MAR} \quad (2.5)$$

Where,

the state X_5 in the above equation represents the output from the integral part of the inverter PI voltage controller,

K_{VII} is the inverter voltage controller integral gain,

V_{IRF} is the inverter direct voltage feedback signal,

V_{REF} is the voltage reference as an external input,

V_{MAR} is the voltage margin as an external input.

$$sX_6 = K_{\gamma II}X_{15} - K_{\gamma II}\gamma_{REF} - K_{II\gamma}\gamma_{MAR}$$

(2.6)

Where,

the state X_6 in the above equation represents the output from the integral part of the inverter PI extinction angle controller, $K_{\gamma II}$ is the inverter extinction angle controller integral gain, γ_{IRF} is the inverter extinction angle feedback signal, γ_{REF} is the extinction angle reference as an external input.

$$sX_7C_{DCL} = -X_1 - X_3$$

(2.7)

Where,

the state X_7 in the above equation represents the voltage across the capacitance in the DC link(V_{CDCL})

The s-domain equivalents of state equations representing the rectifier and inverter side phase locked loop controller are

$$sX_8 = -K_{IPLR}X_9 + K_{IPLR}\phi_{ACR}$$

(2.8)

$$sX_9 = -K_{CPLR}K_{PPLR}X_9 + K_{CPLR}X_8 + K_{CPLR}K_{PPLR}\phi_{ACR}$$

(2.9)

$$sX_{10} = -K_{IPLI}X_{11} + K_{IPLI}\phi_{ACI}$$

(2.10)

$$sX_{11} = -K_{CPLI}K_{PPLI}X_{11} + K_{CPLI}X_{11} + K_{CPLI}K_{PPLI}\phi_{ACI}$$

(2.11)

Where,

the state X_8 and X_{10} in the above equations represents the output from the integral part of the rectifier and inverter phase locked loop controller,

The state X_9 and X_{11} in the above equations represents the output angle from the rectifier (θ_{ACR}) and inverter (θ_{ACI}) phase locked loop controller,

K_{CPLR},K_{PPLR} and K_{IPLR} are the gains of the rectifier side phase locked loop controller,

K_{CPLI},K_{PPLI} and K_{IPLI} are the gains of the rectifier side phase locked loop controller,

ϕ_{ACR} and ϕ_{ACI} is the rectifier and inverter AC voltage phase angle.

The s-domain equivalent of state equations representing the rectifier current transducer, the inverter current transducer, the inverter voltage transducer and the inverter extinction angle transducer (Fig.2. and Fig. 3.) are,

$$sT_{ICRI}X_{12} = -X_{12} + X_1$$

(2.12)

$$sT_{ICRI}X_{13} = -X_{13} + X_3$$

(2.13)

$$sT_{ICRI}X_{14} = -X_{14} + K_{ACI}\varphi_{DCI} + K_{EACI}X_{20} + R_{CRI}X_3$$

(2.14)

$$sT_{ICRI}X_{15} = -X_{15} + C_{ADCI}\varphi_{DCI} + C_{BDCI}X_3 + C_{CDCI}E_{ACI}$$

(2.15)

Where,

T_{ICRI} is the peculiarly added time constant to structure the s-domain equations,γ_{DCI} is the extinction angle.

The linearized coefficientsC_{ADCI},C_{BDCI} andC_{CDCI} are obtained from the equation $cos\gamma_{DCI} = cos\varphi_{DCI} + \frac{\sqrt{2}X_{CRI}I_{DCLI}}{E_{ACI}}$, which gives the relation between the inverter firing angle and the extinction angle.

The s-domain equivalent of state equations for the appropriate firing angle of rectifier φ_{DCR} and inverter φ_{DCI} are expressed as,

$$sT_{RIF}X_{16} = -X_{16} + X_2 + K_{IPR}X_{12} - K_{IPR}I_{REF} + \phi_{ACR} - X_9$$

(2.16)

$$sT_{RIFI}X_{17} = -X_{17} + X_4 + K_{IPI}X_{13} - K_{IPI}I_{REF} + K_{IPI}I_{MAR}$$

(2.17)

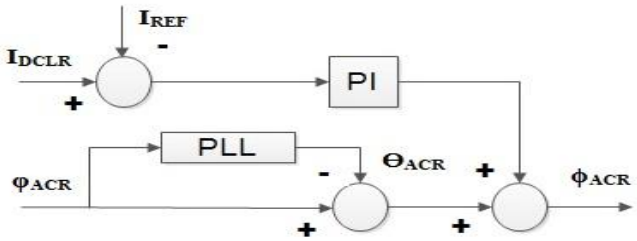

Fig. 2. Control for Rectifier

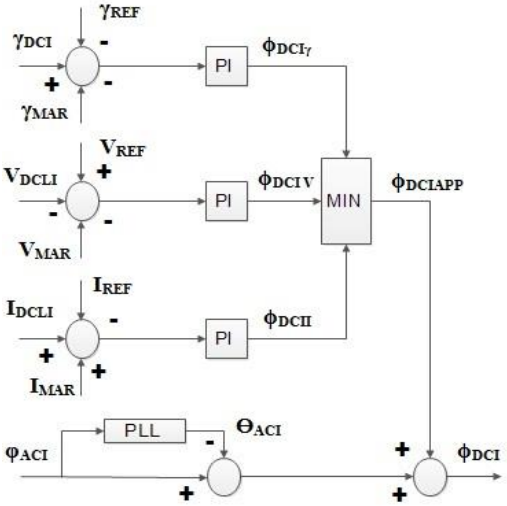

Fig. 3. Control for Inverter

$$sT_{RIFI}X_{18} = -X_{18} + X_5 - K_{VPI}X_{14} + K_{VPI}V_{REF} - K_{VPI}V_{MAR} \quad (2.18)$$

$$sT_{RIFI}X_{19} = -X_{19} + X_6 + K_{\gamma PI}X_{15} - K_{\gamma PI}\gamma_{REF} - K_{\gamma PI}\gamma_{MAR} \quad (2.19)$$

$$sT_{RIF}X_{20} = -X_{20} + \varphi_{DCIAPP} + \phi_{ACI} - X_{11} \quad (2.20)$$

Where,

K_{IPR} is the rectifier current controller proportional gain,

K_{IPI} is the inverter current controller proportional gain,

K_{VPI} is the inverter voltage controller proportional gain,

$K_{\gamma PI}$ is the inverter extinction angle controller proportional gain,

$\varphi_{DCIAPP} = min(\,(\varphi_{DCII}), (\varphi_{DCIV}), (\varphi_{DCI\gamma})),$

φ_{DCII} is the firing angle for inverter derived from current controller output,

φ_{DCIV} is the firing angle for inverter derived from voltage controller output,

$\varphi_{DCI\gamma}$ is the firing angle for inverter derived from extinction angle controller output,

T_{RIF} and T_{RIFI} are the peculiarly added time constants to structure the s-domain equations.

The s-domain equivalent of state equations representing rectifier AC current angle is ψ_{ACR} and inverter AC current angle ψ_{ACI} are expressed as

$$sT_{FRI}X_{21} = -X_{21} + \phi_{ACR} - C_{BACR}X_{16} - C_{CACR}X_1 + C_{DACR}E_{SR} + C_{DACR}E_{SRD} \quad (2.21)$$

$$sT_{FRI}X_{22} = -X_{22} + \phi_{ACI} - C_{BACI}X_{20} - C_{CACI}X_3 + C_{DACI}E_{SI} + C_{DACI}E_{SID} \quad (2.22)$$

Where,

T_{FRI} is the peculiarly added time constant to structure the s-domain equations,

The linearized coefficients C_{BACR} , C_{CACR} and C_{DACR} , for rectifier side are obtained from the equation for AC current angle is $\psi_{ACR} = \Phi_{ACR} - \phi_{ACR}$. In this equation the angle between voltage and current vector is based on the expression of rectifier converter, $cos\Phi_{ACR} = cos\varphi_{ACR} - \frac{R_{CRR}I_{DCLR}\pi}{6\sqrt{3}E_{ACR}}$ and the coefficients $C_{BACI}C_{CACI}$ and C_{DACI} for inverter side are obtained from the equation for AC current angle is $\psi_{ACI} = \Phi_{ACI} - \phi_{ACI}$. In this equation the angle between voltage and current vector is based on the expression of rectifier converter, $cos\Phi_{ACI} = cos\varphi_{ACI} - \frac{R_{CRI}I_{DCLI}\pi}{6\sqrt{3}E_{ACI}}$

Φ_{ACR} and Φ_{ACI} is the rectifier and inverter side AC power phase angle.

The complete state space model for the DC systems is given by,

$$sX_{DCL} = A_{DCL}X_{DCL} + B_{DCLR}U_{DCLR} + B_{DCLI}U_{DCLI} + B_{DCLIN}U_{DCLIN}$$

$$Y_{DCLR} = C_{DCLR}X_{DCL}$$

$$Y_{DCLI} = C_{DCLI}X_{DCL}$$

Where,

A_{DCL}, B_{DCL} and C_{DCL} are obtained from the state equations of the DC network,

$U_{DCLR} = [E_{ACR} \quad \phi_{ACR}]^T$ and $U_{DCLI} = [E_{ACI} \quad \phi_{ACI}]^T$ are the inputs to the DC network from the converter side AC systems which are obtained as given in section B.

$$U_{DCLIN} = [I_{REF} \quad E_{SRD} \quad I_{MAR} \quad V_{REF} \quad \gamma_{REF} \quad E_{SID} \quad \gamma_M \ ]^T$$

$$Y_{DCLR} = [I_{ACR} \quad \psi_{ACR}]^T$$

$$Y_{DCLI} = [I_{ACI} \quad \psi_{ACI}]^T$$

$$X_{DCL} = \begin{bmatrix} I_{DCLR} \\ K_{IIR}(I_{IRF} - I_{REF})/s \\ I_{DCLI} \\ K_{III}(I_{IIF} - I_{REF} + I_{MAR})/s \\ K_{VII}(V_{REF} - V_{VIF} - V_{MAR})/s \\ K_{\gamma II}(\gamma_{\gamma IF} - \gamma_{REF} - \gamma_{MAR})/s \\ V_{CDCL} \\ K_{PLR}(\varphi_{ACR} - \theta_{ACR})/s \\ \theta_{ACR} \\ K_{PLI}(\varphi_{ACI} - \theta_{ACI})/s \\ \theta_{ACI} \\ I_{IRF} \\ I_{IIF} \\ V_{VIF} \\ \gamma_{\gamma IF} \\ \varphi_{DCR} \\ \varphi_{DCII} \\ \varphi_{DCIV} \\ \varphi_{DCI\gamma} \\ \varphi_{DCI} \\ \psi_{ACR} \\ \psi_{ACI} \end{bmatrix}$$

It is required to further transform the input and output matrices from polar coordinate to DQ coordinate frame because DC

system model uses magnitude-angle representation of AC system variables, whereas AC system model is developed in DQ

coordinate frame.

B. Modelling of converter side AC systems

In modelling, the rectifier side AC system is represented by damped L-LR equivalents [11] at fundamental frequency (60 Hz or 50 Hz) and at the third harmonic and the Passive filter of the double tuned type [12] is connected in the source side to eliminate the 11th and 13th order current harmonics along with a second order high pass filter (24th order) and a capacitor for reactive power compensation. The per phase illustration of rectifier side AC system is depicted in Fig. 4. For any phase (R, S and T) of AC system, the states are chosen as the instantaneous values of currents through the inductors and voltages across the capacitors.

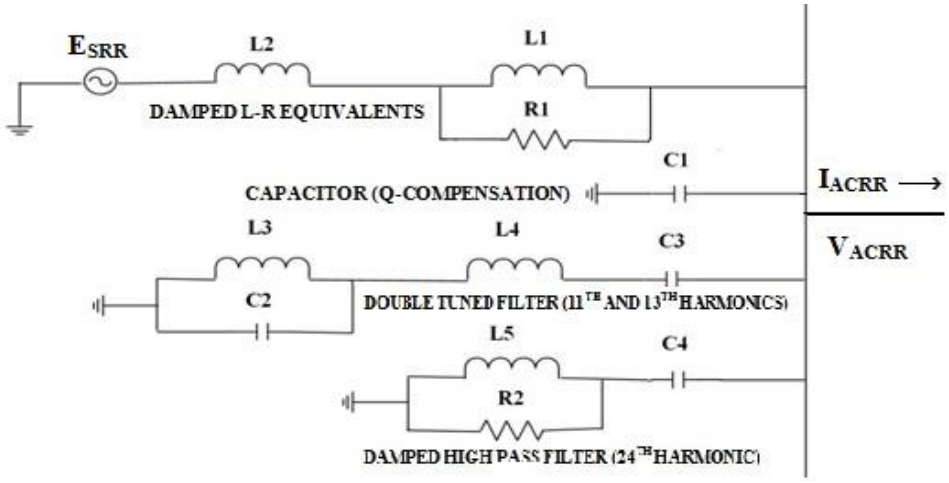

Fig. 4. The per phase equivalent of AC systems.

The s-domain equivalent of the state equations for one of the three phases R are given by,

$$sX_1L_2 = -X_2R_1 + X_1R_1 - X_3 + U_2 \quad (2.23)$$

$$sX_2L_1 = -X_1R_1 + X_2R_1 \quad (2.24)$$

$$sX_3C_1 = -U_1 + X_2 - X_6 - X_8 - \frac{1}{R_2}(X_3 - X_9) \quad (2.25)$$

$$sX_4L_3 = X_5 \quad (2.26)$$

$$sX_5C_2 = X_6 - X_4 \quad (2.27)$$

$$sX_6L_4 = -X_5 - X_7 + X_3 \quad (2.28)$$

$$sX_7C_3 = X_6 \quad (2.29)$$

$$sX_8L_5 = X_3 - X_9 \quad (2.30)$$

$$sX_9C_4 = X_8 + \frac{1}{R_2}(X_3 - X_9) \quad (2.31)$$

The state-space model for phase R is

$$sX_{ACRR} = A_{ACRR}X_{ACRR} + B_{ACRR}U_{ACRR}$$
$$Y_{ACRR} = C_{ACRR}X_{ACRR}$$

Where,

$X_{ACRR} = [I_{L2} \quad I_{L1} \quad V_{ACRR} \quad I_{L3} \quad V_{C2} \quad I_{L4} \quad V_{C3} \quad I_{L5} \quad V_{C4}]$

$U_{ACRR1} = I_{ACRR}$ and $U_{ACRR2} = E_{SRR}$ are the inputs to the model.

$Y_{ACRR} = V_{ACRR}$ is the output of AC bus voltage

A_{ACRR}, B_{ACRR} and C_{ACRR} are obtained from the state equations of the AC system.

The similar approach extended to the remaining phases S and T to obtain the state space model. The complete state space model for the converter side three phase AC systems is given by,

$$sX_{ACR} = A_{ACR}X_{ACR} + B_{ACR}U_{ACR}$$
$$Y_{ACR} = C_{ACR}X_{ACR}$$

Where,

$$X_{ACR} = [X_{ACRR} \quad X_{ACRS} \quad X_{ACRT}]^T$$
$$U_{ACR} = [I_{ACRR} \quad I_{ACRS} \quad I_{ACRT}]^T$$
$$Y_{ACR} = [V_{ACRR} \quad V_{ACRS} \quad V_{ACRT}]^T$$
$$A_{ACR} = \begin{bmatrix} A_{ACRR} & 0 & 0 \\ 0 & A_{ACRS} & 0 \\ 0 & 0 & A_{ACRT} \end{bmatrix}$$
$$B_{ACR} = [B_{ACRR} \quad B_{ACRS} \quad B_{ACRT}]^T$$
$$C_{ACR} = [C_{ACRR} \quad C_{ACRS} \quad C_{ACRT}]$$

To signify the AC system jointly with DC system in the same frequency structure, all the three-phase AC system variables are converted to DQ variables through Park's transformation. The final form of rectifier side AC system model is given by

$$sX_{ACRP} = A_{ACRP}X_{ACRP} + B_{ACRP}U_{ACRP}$$
$$Y_{ACRP} = C_{ACRP}X_{ACRP}$$

Where,

$$U_{ACRP} = [I_{RD} \quad I_{RQ}]^T$$
$$Y_{ACRP} = [V_{RD} \quad V_{RQ}]^T$$

The above model takes DQ components of corresponding current and voltage as inputs and outputs, respectively. The model inputs are obtained from the AC system model, whereas the model outputs are used as inputs for the DC system model. The complete state space model for the inverter side three phase AC systems is obtained by the similar procedure used for the modelling of rectifier side AC systems.

III. SIMULATION RESULTS AND DISCUSSION

The HVDC transmission systems model is implemented in the working platform of MATLAB/Simulink adapting above mentioned range of features based on the data in [13] with essential modifications, and it is simulated for duration of 2 second to observe the steady state performance. There were some initial transients that subsided within about 0.5 sec and the system reached steady state. The rectifier side AC voltage and current, the rectifier DC voltage and current, the rectifier firing angle (alpha) are shown in the Fig. 5.

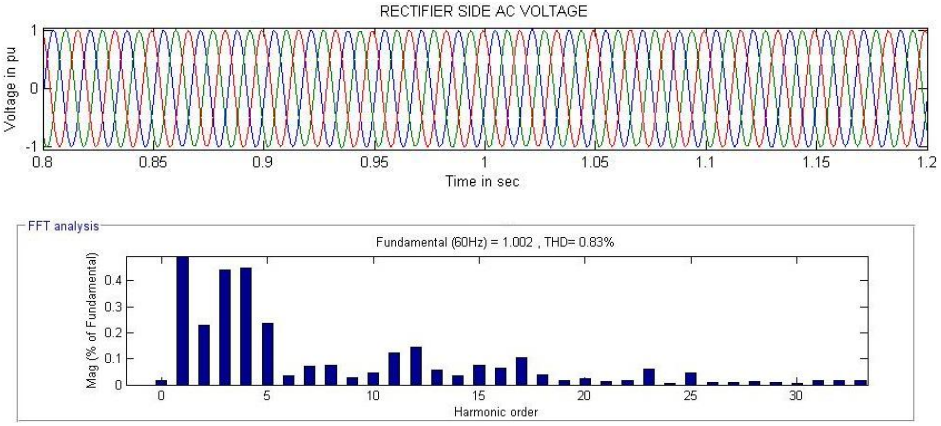

Fig. 5(a). Rectifier side AC voltage and its harmonics spectrum

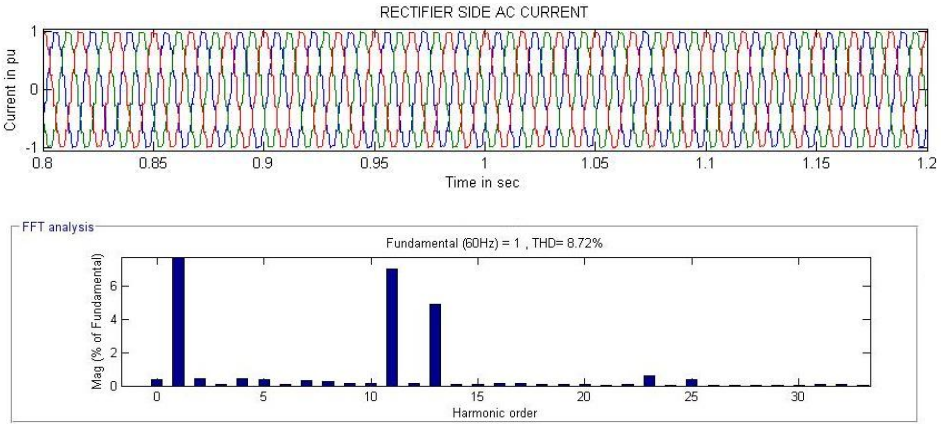

Fig. 5(b). Rectifier side AC current and its harmonics spectrum

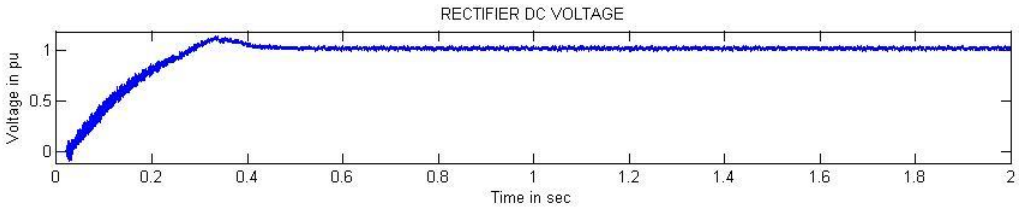

Fig. 5(c). Rectifier DC voltage

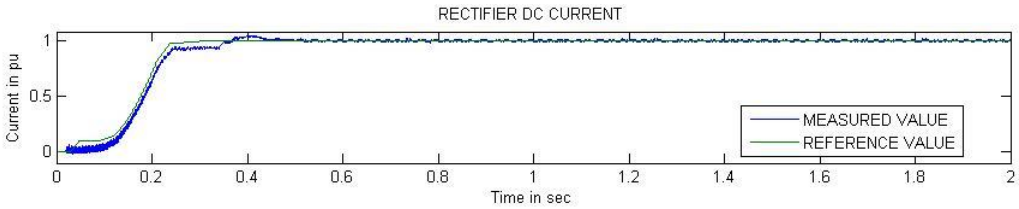

Fig. 5(d). Rectifier DC current

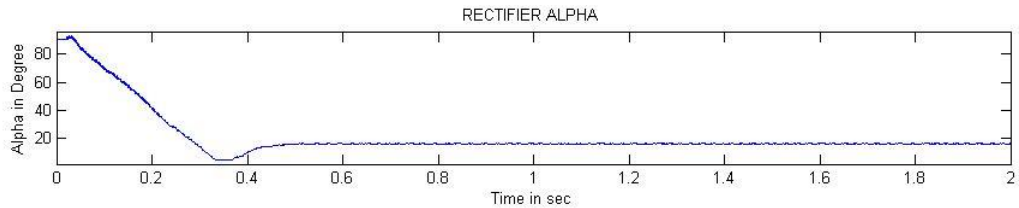

Fig. 5(e). Rectifier firing angle (alpha)

From the rectifier side AC waveforms and their harmonic spectrum, it is found that voltage and current are equal to 1 p.u. and the 11^{th} and 13^{th} harmonics are the dominant harmonics on rectifier side. From the DC waveforms on the rectifier, the DC voltage and current show small oscillations around the reference value (1 p.u.). The mean of output DC voltage and current are 1.0 p.u. At steady state, the measured firing angle is around 16.5 degrees on the rectifier side. The rectifier side firing angle is purely depending on the current controller since the rectifier is controlled by the current controller alone.

The inverter side AC voltage and current, the inverter DC voltage and current, the inverter angle extinction angle, the inverter firing angle from various controls, the inverter firing angle alpha are shown in the Fig. 6.

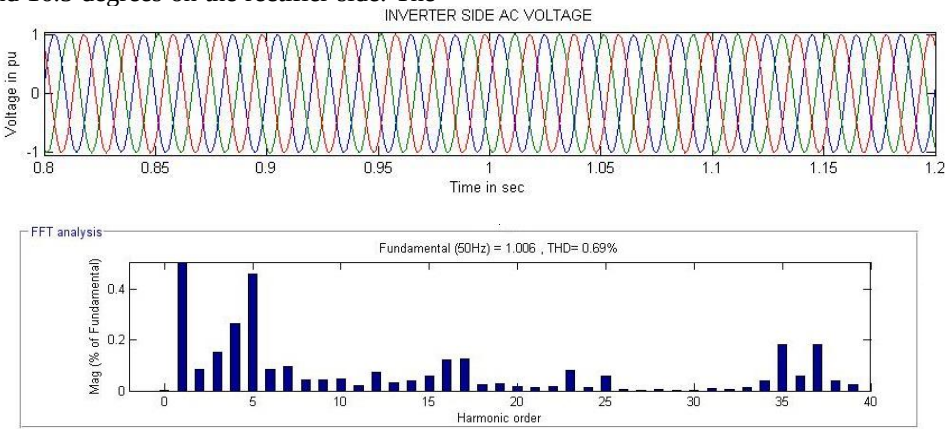

Fig. 6(a). Inverter side AC voltage and its harmonics spectrum

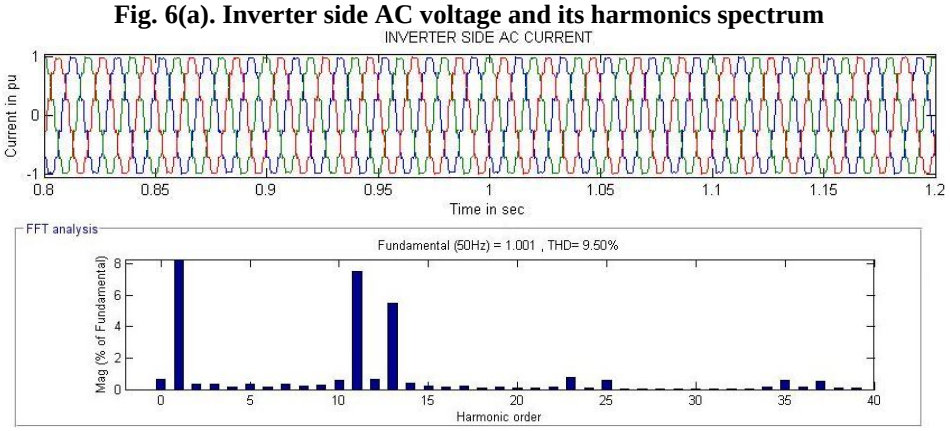

Fig. 6(b). Inverter side AC current and its harmonics spectrum

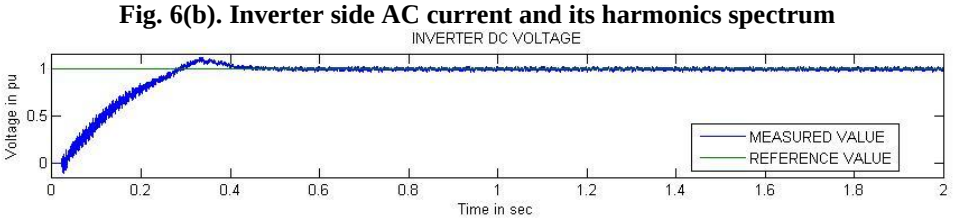

Fig. 6(c). Inverter DC voltage

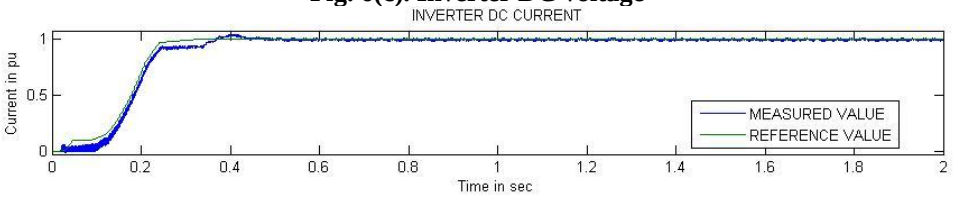

Fig. 6(d). Inverter DC current

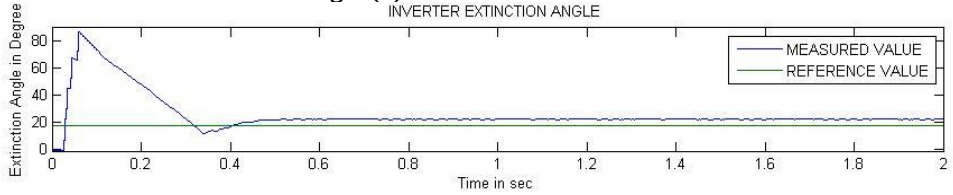

Fig. 6(e). Inverter extinction angle

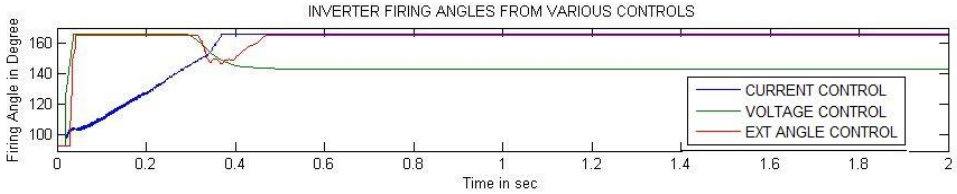

Fig. 6(f). Inverter firing angle from various controls

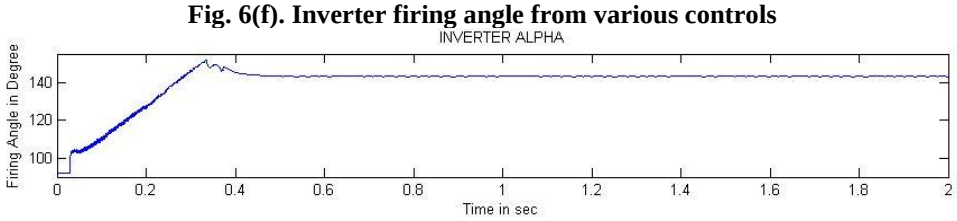

Fig. 6(g). Inverter firing angle (alpha)

From the inverter side AC waveforms and their harmonic spectrum, it is found that voltage and current are equal to 1 p.u. and the 11^{th} and 13^{th} harmonics are the foremost harmonics on inverter side. As of the DC waveforms on the inverter, the DC voltage and current show small oscillations around the reference value (1 p.u.). The mean of output DC voltage and current are 1.0 p.u. At steady state, the measured firing angle is approximately 143 degrees on the inverter side. Since the inverter is controlled by three controllers namely current controller, voltage controller and extinction angle controller. so, the inverter firing angle is decided by the minimum value of firing angle from the three individual controllers. From the inverter firing angle waveform, it is evident that voltage controller has significant role in determining the inverter firing angle.

IV. CONCLUSION

This paper has evidently established a well-developed linear continuous model of current source converter based twelve pulse HVDC transmission systems. This involvement can be very useful for designing and safeguarding persons, for analyzing the operation of the HVDC system under different operating environment to optimize the performance. The HVDC transmission system model is implemented in the MATLAB/Simulink environment and operation of the system is investigated by observing the rectifier side AC quantities, rectifier DC quantities, inverter side AC quantities and inverter DC quantities. Simulation results show that linear continuous model has tolerable accuracy.

ACKNOWLEDGMENT

The authors gratefully acknowledge the support and facilities provided by the authorities of Government College of Engineering, Dharmapuri, Government Polytechnic College, Ariyalur and Annamalai University, Annamalainagar, Tamilnadu, India to carry out this research work.

REFERENCES

1. O.Peake, “The History of High Voltage Direct Current Transmission”, Australasian Engineering Heritage Conference, pp.1-8, 2009.
2. K. Meah, S. Ula, “Comparative Evaluation of HVDC and HVAC Transmission Systems”, IEEE General Meeting on Power Engineering Society, pp.1-5, 2007.
3. V, G. Agelidis, G. D. Demetriades, N. Flourentzou, “Recent Advances in High-Voltage Direct-Current Power Transmission Systems”, IEEE International Conference on Industrial Technology (ICIT), 2006, pp.206-213.
4. Bahrman.M.P, “HVDC transmission overview”, IEEE Transmission and Distribution Conference and Exposition, pp.1-7, 2008.
5. Lorden.D.J, Clark.K, Larsen.E.V, “A Digitally based HVDC Firing-Pulse Synchronization Control-Description and Model Development”, IEEE Transactions on Power Delivery, Vol. 7, No. 3, pp. 1405-1414, 1992.
6. Huang.G.A, Krishnaswamy, “HVDC Controls for Power System Stability”, IEEE Power Engineering Society Summer Meeting, Vol. 1, pp. 597-602, 2002.
7. Hazra.J, Phulpin.Y, Ernst.D, “HVDC Control Strategies to Improve Transient Stability in Interconnected Power Systems”, IEEE Power Tech, Bucharest, pp.1-6, 2009.
8. Szechtman.M, Wess.T, Thio.C.V, “A Benchmark Model for HVDC System Studies”, IEEE International Conference on AC and DC Power Transmission, pp.374-378, 1991.
9. D.Jovcic, N.Pahalawaththa, M.Zavahir, “Analytical modelling of HVDC-HVAC system”, IEEE Transactions on Power Delivery, Vol. 14, No. 2, pp. 506-511, 1999.
10. K.R.Padiyar, “HVDC Power Transmission Systems”, New Age International (P) Limited Publishers, Delhi, 1993.
11. M. Khatir, S A. Zidi, S. Hadjeri, M K. Fellah, R. Amiri, "Performance Evaluation of Line and Capacitor Commutated Converter based HVDC System in Simulink Environment", Journal of Electrical & Electronics Engineering, Vol. 8, No. 8, pp. 481-490, 2008.
12. Xiao Yao, “Algorithm for Parameters of Double Tuned Filter”, IEEE Conference on Harmonic and Quality of Power (PEcon), Greece, Vol. 1, pp.1 54-157, 1998.
13. Christian Dufour, Jean Mahseredjian, Jean Belanger “A Combined State-Space Nodal Method for the Simulation of Power System Transients”, IEEE Transactions on Power Delivery, Vol. 26, No. 2, pp. 928-935, 2011.

AUTHORS PROFILE

Dr.S.Seenivasan received Bachelor of Engineering in Electrical and Electronics in 2005, Master of Engineering in Power System in 2011 and Ph.D in Electrical Engineering in 2016 from Annamalai University, Annamalainagar, Tamilnadu, India. At present, he is an Assistant Professor in the Department of Electrical Engineering at Government College of Engineering, Dharmapuri. He has published more than 25 papers in international journals. His research interests are in high voltage DC transmission systems and soft computing techniques.

Dr.S.Vadivel received Bachelor of Engineering in Electrical and Electronics in 2007, Master of Engineering in Power System in 2011 and Ph.D in Electrical Engineering in 2018 from Annamalai University, Annamalainagar, Tamilnadu, India. At present, he is a Lecturer in the Department of Electrical Engineering at Government Polytechnic College, Ariyalur. He has published more than 15 papers in international journals. His research interests are in power system and D-FACTS.